Bioresource Technology 388 (2023) 129724

Contents lists available at ScienceDirect

Bioresource Technology

journal homepage: www.elsevier.com/locate/biortech

Green solvents to enhance hydrochar quality and clarify effects of secondary char

Giulia Ischia [a,b], Jillian L. Goldfarb [b,c], Antonio Miotello [d], Luca Fiori [a,e,*]

[a] Department of Civil, Environmental and Mechanical Engineering, University of Trento, Via Mesiano 77, 38123 Trento, Italy
[b] Department of Biological and Environmental Engineering, Cornell University, Ithaca, NY 14853, USA
[c] Smith School of Chemical and Biomolecular Engineering, Cornell University, Ithaca, NY 14853, USA
[d] Department of Physics, University of Trento, Via Sommarive 14, 38123 Trento, Italy
[e] Center Agriculture Food Environment (C3A), University of Trento, San Michele all'Adige, 38010 Trento, Italy

HIGHLIGHTS

- Polar solvents effectively remove polar organics adsorbed on the hydrochars.
- Adsorbed organics confer to hydrochars low thermal stability at low temperatures.
- Solvent extraction is effective in improving hydrochar quality.
- The composition of the extractable phase resembles that of the HTC liquor.
- Polar solvents do not dissolve secondary char (carbonaceous microspheres)

GRAPHICAL ABSTRACT

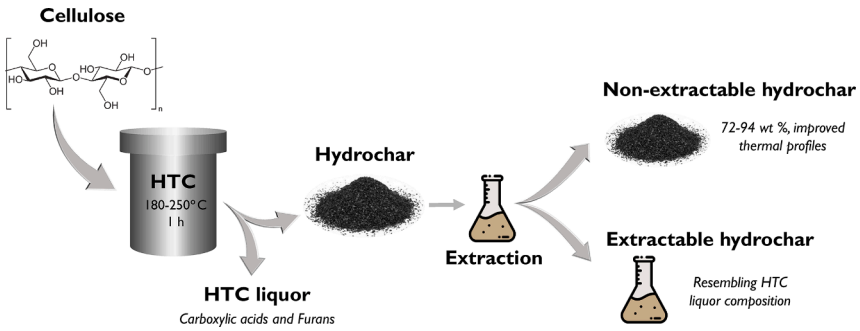

ARTICLE INFO

Keywords:
Hydrothermal carbonization
HTC
Solvent extraction
Thermal stability
Cellulose

ABSTRACT

Several limitations hinder the industrial-scale implementation of hydrothermal carbonization (HTC) of biomass, especially the quality of as-carbonized hydrochar. This work investigates solvent extraction of hydrochars to enhance their potential applications. Hydrochars were produced at several HTC temperatures (190, 220, 250 °C) from cellulose and extracted using combinations of green polar solvents (ethyl acetate, acetone, and methanol). Results show that the composition of the extractable fraction resembles that of the HTC liquor, rich in carboxylic acids and furan derivatives, while the non-extractable solid phase shows improved thermal profiles devoid of highly volatile compounds. Carbon microspheres (non-dissolvable secondary char) are unaffected by extraction. The organics adsorbed on the hydrochar surface comprise highly volatile species and solvent washing effectively removes them.

1. Introduction

Hydrothermal carbonization (HTC) for biomass valorization is now used at pilot and industrial-scale plants. The unique properties of water under high temperature and pressure (180–250 °C and 10–50 bar) enable the conversion of wet biomass into a solid carbonaceous phase (i.

* Corresponding author at: Department of Civil, Environmental and Mechanical Engineering, University of Trento, Via Mesiano 77, 38123 Trento, Italy.
E-mail address: luca.fiori@unitn.it (L. Fiori).

https://doi.org/10.1016/j.biortech.2023.129724
Received 12 June 2023; Received in revised form 14 August 2023; Accepted 5 September 2023
Available online 6 September 2023
0960-8524/© 2023 The Authors. Published by Elsevier Ltd. This is an open access article under the CC BY license (http://creativecommons.org/licenses/by/4.0/).

e., hydrochar), an organic-laden liquid phase, and a gas phase. HTC can treat a diverse range of heterogeneous and wet substrates (like organic wastes and sewage sludge) as a standalone waste management strategy and as part of an integrated biorefinery for producing materials with high added value (Gong et al., 2022). Added-value materials include solid biofuels, soil amendments, and feedstocks for activated carbons for conversion into electrodes, composite catalysts, or adsorbents (Nicolae et al., 2020).

However, products of HTC face several limitations. For example, the hydrochar and aqueous phase show potential phytotoxicity and are therefore questionable soil amendments (Karatas et al., 2022). The as-carbonized hydrochar has a low surface area and a high reactivity at low temperatures, limiting its usefulness as an adsorbent and solid biofuel in combustion applications (Nguyen et al., 2022). To overcome hydrochar limitations, prior researchers investigated pre- and post-treatments integrated into HTC, including thermal treatments (e.g. torrefaction and pyrolysis), solvent extraction, and chemical/physical activation (Nicolae et al., 2020). Benavente et al. (2022) recently demonstrated that treating microalgae with solvents prior to HTC helps to reduce the phytotoxic potential of hydrochar.

Hydrochar solvent extraction has several potentialities. It improves hydrochar thermal decomposition profiles (Ischia et al., 2021; Lucian et al., 2018; Pecchi et al., 2022), and reduces potential adverse effects on plant growth by transferring phytotoxic compounds from the solid to the solvent phase (Karatas et al., 2022). Solvent extraction also recovers target compounds (like phenols and furfural) from the hydrochar surface (Arauzo et al., 2020a; Wu et al., 2020). To be feasible at industrial scale, the extraction stage must be optimized according to the desired target products and be as green as possible. Indeed, it could be environmentally problematic since it requires an organic solvent and produces a wastewater/solvent stream. Adopting recognized green solvents is crucial for developing a sustainable biorefinery.

Despite its potential, there are few studies that investigate solvent extraction of hydrochar. The present work extracts hydrochar with green solvents as a post-treatment step to remove species that confer unwanted properties like high reactivity and phytotoxicity. Further, this study probes the causes behind the low thermal stability of hydrochars at low temperatures, for which a certain degree of uncertainty in the current scientific literature can be observed. Indeed, some studies attribute the high instability and reactivity to microspheres produced from the re-polymerization of organics in process water released from the parent biomass back onto the biomass, often termed secondary char (Benavente et al., 2022; Gao et al., 2019). However, depending on the parent feedstock composition, some of these microspheres (in particular those from pure feedstocks such as glucose) have a high degree of carbonization and aromatization (Gong et al., 2022; Ischia et al., 2022), which makes the spheres thermally stable. For heterogeneous biomass feedstocks, organics that are released into the process water and then adsorb on the hydrochar surface generally have high volatility and are likely responsible for the high reactivity and phytotoxicity (Benavente et al., 2022; Karatas et al., 2022). These characteristics make the removal of such compounds particularly appealing to enhance potential for agricultural applications of the solid hydrochar. In the present work, "secondary char" refers only to the carbonaceous microspheres, likely derived from the recombination/repolymerization of reactive fragments dissolved into the HTC liquid phase (Falco et al., 2011; Gong et al., 2022), that remain on the hydrochar surface after extraction of the volatile organics. Owing to the well-defined spherical morphology and tunable properties of secondary char, proposed applications include as a precursor of sustainable multifunctional carbon materials (Nicolae et al., 2020) for upconversion to supercapacitors, electrodes, gas capture, electrocatalysts, and adsorption (Gong et al., 2022; Modugno and Titirici, 2021).

This work systematically investigates the solvent extractions of hydrochars made from cellulose. Cellulose was chosen as a model substrate for investigation as its HTC reaction mechanisms are well documented and it is a building block of carbohydrates and lignocellulosic biomasses. Cellulose represents a significant fraction of common biomasses (up to 40–45 % for lignocellulosic biomass, and up to 50 % in grass). For this reason, it is often considered an ideal model compound for investigation, and significant literature exists for comparative analyses (Cao et al., 2021).

The solvents chosen are ethyl acetate, acetone, and methanol, which are relatively polar, are recognized as green solvents and are rated low-risk solvents (Yilmaz and Soylak, 2020). These aspects are crucial for satisfying the environmental requirements needed for industrial-scale plants. Analyses were performed on the non-extractable hydrochar (i.e., the washed solid phase) and the extracts, demonstrating the efficacy of the proposed solvent extraction in improving hydrochar properties.

2. Material and methods

2.1. Hydrothermal runs

Hydrothermal runs were performed on microcrystalline cellulose powder (Alfa Aesar, minimum 97% pure). For each HTC run, 30 g of cellulose plus 150 mL of distilled water were added to a 300 mL hydrothermal reactor (Parr, stirred, 350 °C, 5000 psi). Tests were performed at 190, 220, and 250 °C at a residence time of 1 h. Reaction time commenced after the heating phase (which itself lasted 20–30 min) was complete. Before every test, the reactor was flushed three times with pure nitrogen to guarantee an inert environment, while during the run the reactor contents were homogenized using a stirrer at 300 rpm. After the reaction time passed, the reactor was cooled down by immersion in a cold-water bath. The mass of gas produced in the reaction was measured by weighing the reactor before and after venting the gas post-HTC after the reactor reached room temperature. The liquid fraction was separated from the solid phase through a qualitative filter at 2.5 μm. The solid phase (hydrochar) was recovered and dried overnight at 105 °C in a ventilated oven. The amount of biomass dissolved in the liquid phase was computed by difference. The mass yields were computed as the ratio between the solid/gas/liquid phase and the amount of starting feedstock. HTC runs were repeated at least twice.

2.2. Solvent extraction

Cellulose and hydrochars were extracted with *n*-hexane (purchased from Sigma-Aldrich, > 97 % purity) to evaluate the presence of extractable non-polar compounds. Then, cellulose and hydrochars were extracted using ethyl acetate, acetone, and methanol (HPLC grade, purity 99.9 %, purchased from Alfa Aesar). These solvents are all polar/slightly polar: ethyl acetate is the least polar, acetone is polar protic, and methanol polar aprotic, with dielectric constants of 6.02, 20.7, and 33, respectively (Byrne et al., 2016; "PubChem," n.d.). Four sets of extractions were performed: ethyl acetate alone (E1); a 1:1 vol mixture of acetone and methanol (E2); a 1:1:1 vol mixture of ethyl acetate, acetone and methanol (E3); sequential extraction with ethyl acetate followed by extraction with a 1:1 vol mixture of acetone and methanol (E4). Ethyl acetate, acetone, and methanol were selected as they are considered greener than many alternatives and exhibit vary degrees of polarity but with slight differences among properties such as density and dielectric constant (Byrne et al., 2016). Given the lack of literature regarding solvent extraction, the solvent ratios were set to have equal volume to assess the combination of different solvent properties.

Extractions were performed by contacting 2 g of dry material with 40 mL of solvent mixture in a beaker and mixed for 12 h on a shaking table. An excess of solvent was used to ensure the complete dissolution of soluble compounds. After shaking, the solid phase (i.e., the non-extractable hydrochar) was separated from the liquid phase (i.e., the solvent with the hydrochar extractable phase) through 2.5 μm qualitative cellulose filter paper. The non-extractable solid hydrochar was dried overnight at 105 °C to evaporate residual solvent. The solvent

containing the extracted compounds was stored in a fridge at 4 °C before analysis. Each extraction was repeated at least three times.

To provide further insights on secondary char, glucose hydrochars produced at 250 and 270 °C carbonized for 1 h in previous work (Ischia et al., 2022) were extracted with E2 (1:1 acetone:methanol). These samples have the advantage of consisting only of secondary char as glucose, under the conditions tested, is completely dissolved in water before the HTC run, and therefore does not form any primary char.

For each extraction, the "extracted solid yield" (SY) was computed as the ratio between the amount of hydrochar remaining after extraction (non-extractable HC, $m_{HC,nex}$) and the amount of hydrochar before the extraction (m_{HC}), expressed in percentage terms (Eq. (1)). The "extraction yield" (EY) was calculated as the ratio between the amount of hydrochar extracted and the amount of hydrochar before the extraction, expressed in percentage terms (Eq. (2)).

$$\text{Extr. Solid Yield (SY)} = \frac{m_{hc,nex}}{m_{HC}} \bullet 100\% \quad (1)$$

$$\text{Extr. Yield (EY)} = \frac{m_{HC} - m_{HC,nex}}{m_{HC}} \bullet 100\% = 100\% - SY \quad (2)$$

Finally, the "carbon loss" (CL) due to extraction was computed as the ratio of the mass of carbon extracted into the solvent and the amount of carbon in the hydrochar before extraction (Eq. (3)).

$$CL = \frac{C_{HC} - C_{HC,nex}\, SY/100}{C_{HC}} \quad (3)$$

Where C_{HC} and $C_{HC,nex}$ are the weight percentage of carbon (data from ultimate analysis, Section 2.3) in the hydrochar before extraction and after extraction, respectively.

2.3. Solid analysis

Ultimate analyses were performed using a CE-440 Elemental Analyzer (Exeter Analytical) to determine carbon (C), hydrogen (H), and nitrogen (N) contents, calibrated using sulfanilamide and following the ASTM D-5373 standard method. Tests were performed at least in triplicate and oxygen (O) was computed by difference.

The higher heating value (HHV) of the dried hydrochars was computed by applying the Dulong's correlation (Eq. (4)).

$$HHV = 33.6 \bullet C\% + 141.8 \bullet H\% - 14.5 \bullet O\% \quad (4)$$

Proximate analysis on hydrochars from cellulose was performed on a TA Instruments 5550 Thermogravimetric Analyzer. Between 2 and 8 mg of dry sample were placed into a 70 μL alumina crucible, heated in high purity nitrogen at 10 °C/min up to 110 °C and held for 30 min to remove moisture, then at 10 °C/min from 110 to 900 °C and held for 30 min to determine volatile matter (VM). Then, samples were heated from 900 to 950 °C under dry air and held for 30 min with the loss attributed to fixed carbon (FC). Residual matter remaining after oxidation is loosely termed "ash." Analyses on hydrochars from glucose were performed on 6 mg of samples using a Q5000 IR thermogravimetric analyzer (TA Instruments-Waters LLC), at a heating rate of 10 °C/min flushing nitrogen at 15 mL/min.

To gauge the thermal stability of the hydrochars, the extent of sample converted at any time t, x(t), during the pyrolytic step (heating until 900 °C under N_2) was computed as:

$$x(t) = \frac{m_{dry} - m_t}{m_{dry} - m_{pyr}} \quad (5)$$

where m_{dry} is the mass of the dry sample, m_t the mass at any time t, and m_{pyr} the residual mass left at the end of the pyrolytic step. Derivative thermogravimetric (DTG) conversion curves were constructed by plotting dx/dt versus temperature.

The hydrochar morphology was investigated using a JEOL JSM-7001F Field Emission Scanning Electron Microscope (SEM) with an electron beam energy of 5–15 keV. Samples were coated with gold before analysis.

2.4. HTC liquor analysis

The composition of the liquid phases (HTC liquor and extracts) was investigated using a Shimadzu High-Performance Liquid Chromatography (HPLC) equipped with an Ultra Aqueous C18 Column. The column was operated at 30 °C at a total flow rate of 1.5 mL/min. The mobile phase consisted of a 10 mM solution (pH 2.6) of phosphoric acid and acetonitrile (90/10 in the first 10 min and 70/30 from 10 to 50 min). The detection was performed through a UV–Vis Detector (SPD-20A) set at a wavelength of 210 nm. HPLC was calibrated using 14 HPLC-grade compounds: glycolic acid (1.256 min), formic acid (1.370 min), lactic acid (1.370 min), propionic acid (1.370 min), levulinic acid (2.470 min), acetic acid (2.741 min), 2(5H) furanone (2.357 min), 5-HMF (3.329 min), furfural (5.418 min), 5-methylfurfural (11.479 min), 1,3 cyclopentanedione (2.575 min), 2-cyclopenten-1-one (4.215 min), phenol (11.980 min), 2,6 dimethoxyphenol (18.157 min). The sum of HPLC compounds (their mass computed considering their concentration and molar mass) divided by the amount of initial cellulose was referred to as "HPLC yield" and it was compared with the HTC liquid yield and the extraction yield computed by Eq. (2). Anecdotally, the HPLC column used in this work needed significant backwashing and experienced a shorter overall lifetime due to irreversible pressure loss, potentially due to fouling by colloidal particles. Then, the total amount of carbon detected through HPLC (TOC_{HPLC}) was computed as the sum of the C concentration (g/L) of each compound.

The total organic carbon (TOC) of the HTC liquor was measured using an automated Shimadzu TOC-L CSH (with TNM-L unit addition) according to ASTM D7573.

3. Results and discussion

3.1. Hydrochar from cellulose

As HTC temperature increases, cellulose undergoes a progressive volatile matter loss and aromatization of the residual biomass (Falco et al., 2011), and a significant degradation occurs at T ≥ 220 °C (Table 1). Degrading cellulose below 200–220 °C is difficult due to the strong β-(1–4) glycosidic bonds between the glucose monomers comprising cellulose (Gong et al., 2022). At an HTC temperature of 190 °C, cellulose properties are almost unaffected. The hydrochar mass yield is 91.8 wt% (Table 1) with minimal gas formation (Supplementary Information) owing mainly to limited hydrolysis reactions. The hydrochar composition (Table 1) and DTG curves (Fig. 1) resemble the raw cellulose, with a slight shift of the DTG peak towards higher temperatures (from 345 to 355 °C). At HTC temperatures of 220 and 250 °C, cellulose undergoes a significant decomposition, with the hydrochar yield as low as 47.6 % at 250 °C. Higher temperatures favor reactions like carbonylation and decarboxylation which resulted in gas yields increasing from 0.8 to 5.7 to 9.2 wt% ($p < 0.05$, unpaired tailed *t*-test between neighboring points) as HTC temperature increased from 190 to 220 to 250 °C, respectively. The increasing elemental carbon of the hydrochar is responsible for HHV enhancement, which changes from 15.9 to 25.4 MJ/kg as HTC temperature goes from 190 to 250 °C (Table 1). The carbon–carbon bond concentration – seen through a highly statistically significant decrease in the H/C and O/C ratios between 190 and 220 °C in Table 1 ($p < 0.01$, two-tailed *t*-test) – suggests that the hydrochar undergoes significant dehydration, deoxygenation and decarboxylation reactions (to form either saturated C-C or unsaturated C=C bonds (Gong et al., 2022)). The differences in H/C and O/C ratios between 220 and 250 °C are not statistically significant, but the increase in carbon concentration from 65.1 wt% to 68.8 wt% is significant ($p < 0.05$) as is the corresponding decrease in oxygen.

DTG curves (Fig. 1) show that higher HTC temperatures enhance the

Table 1
Effect of hydrochar extractions on extraction solid yield, composition (proximate and ultimate), carbon loss, hydrogen and oxygen to carbon atomic ratios, and HHV. "HTC → Extr" refers to the combination of HTC and extraction. Confidence intervals represent standard deviations computed from error propagation (in details for solid yields, for proximate < 1.2 %, ultimate < 0.4 %, CL < 3.6 %, H/C and O/C < 0.05, HHVs < 0.3 MJ/kg). (*by difference).

Sample		Solid yield (wt %)		Proximate (wt %)		Ultimate (wt %)				CL (%)	O/C (-)	H/C (-)	HHV (MJ/kg)
		Extr.	HTC → Extr.	FC	VM	C	H	N	O*				
Cellulose		100.0 ± 0.1	100.0 ± 0.1	3.4	96.6	40.1	6.3	0.3	53.3	-	1.0	1.9	14.7
190 °C	HC	–	91.8 ± 0.6	5.0	95.1	43.1	6.2	0.3	50.5	-	0.9	1.7	15.9
	E1	93.2 ± 0.9	85.5 ± 1.4	7.3	92.7	44.9	6.1	0.2	48.8	−3.0	0.8	1.6	16.7
	E2	95.5 ± 1.0	87.7 ± 1.5	4.6	95.4	43.5	6.5	0.3	49.7	−3.5	0.9	1.8	16.6
	E3	94.9 ± 0.9	87.1 ± 1.4	5.5	94.5	43.2	6.3	0.3	50.2	−4.9	0.9	1.8	16.2
	E4	93.0 ± 0.9	85.4 ± 1.4	5.9	94.1	43.4	6.2	0.4	50.0	−6.4	0.9	1.7	16.1
220 °C	HC	–	54.9 ± 0.7	40.3	59.7	65.1	4.8	0.2	29.9	–	0.3	0.9	24.3
	E1	92.0 ± 1.4	50.5 ± 1.4	42.6	57.4	64.8	4.5	0.2	30.4	−8.3	0.4	0.8	23.7
	E2	85.0 ± 1.3	46.7 ± 1.3	52.0	48.0	67.9	3.9	0.2	28.1	−11.3	0.3	0.7	24.2
	E3	74.0 ± 1.3	40.6 ± 1.3	37.2	62.8	60.2	4.9	0.2	34.7	−31.5	0.4	1.0	22.2
	E4	72.0 ± 1.1	39.5 ± 1.1	32.0	68.0	55.8	5.6	0.3	38.3	−38.2	0.5	1.2	21.2
250 °C	HC	–	47.6 ± 1.0	47.8	52.2	68.8	4.3	0.2	26.7	–	0.3	0.8	25.4
	E1	91.5 ± 1.8	43.6 ± 1.8	51.2	48.8	69.1	4.3	0.3	26.3	−8.1	0.3	0.7	25.5
	E2	91.5 ± 1.4	43.5 ± 1.6	52.0	48.0	68.8	4.3	0.2	26.6	−8.6	0.3	0.8	25.4
	E3	90.1 ± 1.4	42.9 ± 1.5	51.3	48.7	68.7	4.2	0.2	26.9	−9.9	0.3	0.7	25.1
	E4	90.0 ± 1.4	42.8 ± 1.5	53.2	46.8	67.0	4.2	0.3	28.5	−12.4	0.3	0.8	24.3

thermal stability of the material. Indeed, the decomposition peak shifts towards higher temperatures and lower mass loss rate as HTC temperature increases. DTG curves provide insight into the mechanism behind the decomposition, which can be approximately divided into three stages: stage I at 140–280 °C, stage II centered at 345–355 °C, and stage III centered at 425 °C.

At 140–280 °C (stage I), all the hydrochar thermal profiles slightly depart from that of raw cellulose, suggesting the presence of new volatile species formed through HTC (Fig. 1 (b)). These species likely consist of organics present in the liquid environment of the HTC reaction that accumulate and are adsorbed on the hydrochar surface. The 190 and 220 °C hydrochars show a decomposition peak centered at 345–355 °C (stage II), similar to that of cellulose occurring at 345 °C. The overlapping of stage II with the thermal profile of raw cellulose suggests that a fraction of partially unreacted cellulose is still present, indicating that the HTC operating condition of 220 °C is too mild to complete decomposition of its structure. The presence of partially unreacted cellulose at 220–225 °C was also observed in previous literature through ^{13}C NMR and ^{1}H NMR spectra (Arauzo et al., 2020b) as well as DTG curves (Kang et al., 2012). The 220 and 250 °C hydrochars exhibit a peak centered at 425 °C (stage III), not present for raw cellulose or the 190 °C hydrochar. As HTC temperature increases, the cellulosic fraction progressively undergoes bulk carbonization reactions that rearrange the inter- and intra-molecular structure, condensing the carbon, as noted through the elemental analysis. It is likely that aromatic bonds are formed at higher HTC temperatures as aromatic structures would impart higher thermal stability and the appearance of a third decomposition stage. Indeed, at an HTC temperature of 250 °C, stage II completely disappears in favor of a single decomposition peak centered at 425 °C (stage III). The literature confirms that an increase in HTC temperature results in the formation of a more significant number of aromatic structures (Falco et al., 2011; He et al., 2022), which improve thermal stability.

Carbon microspheres that derive from the repolymerization of organics and form the secondary char likely pyrolyze during stage III of the DTG curves. Indeed, DTG curves of pristine microspheres from the HTC of glucose produced previously (Ischia et al., 2022) show that their principal DTG peak occurs at 425 °C, as shown in Fig. 2. Similar results were observed also by Kruse and Zevaco (2018), who demonstrated that microspheres produced from pure 5-HMF (the key reaction intermediate between glucose and secondary char) decompose above 400 °C. Furthermore, the extraction process has no impact on the DTG peak of pure secondary char (Fig. 2), indicating its greater thermal stability compared to other hydrochar fractions. The decomposition shoulder attributed to organics (stage I) noticeably decreases after the extraction process (Fig. 2); this supports the cellulose hydrochar observations.

SEM images of the hydrochars (Supplementary Information) show that microspheres present on the hydrochar surface remain (qualitatively) the same after extraction. Therefore, it is unlikely that the microspheres are responsible for the low thermal stability of the as-carbonized hydrochars. Further, it is plausible that these microspheres have an aromatic structure that enhances the thermal stability of the solid hydrochar post-extraction. Future work could probe the composition and structure of the microspheres to confirm this explanation.

3.2. HTC liquor

Carboxylic acids and furan derivatives constitute the main fractions of the HTC liquor at all carbonization temperatures; small quantities of ketones and phenols emerge at higher temperatures (Fig. 3). The carboxylic acids mainly derive from the degradation of cellulosic monomers released like fructose and glucose. Glycolic acid, produced from the oxidation of fructose intermediates, represents the largest fraction of carboxylic acids (26.2–30.3 mg/$g_{cellulose}$). Levulinic acid, relatively abundant, derives from the rehydration of 5-HMF. The concentration of levulinic acid decreases from 220 °C to 250 °C, likely because it participates in the formation of the secondary char's carbon microspheres (Falco et al., 2011). The concentrations of lactic acid and propionic acid peak at 220 °C and then decrease at 250 °C, as they degrade to ethanol and acetic acid, respectively (Poerschmann et al., 2017).

5-HMF derives from the rehydration of sugar monomers dissolved into the aqueous phase. As a reaction intermediate, 5-HMF shows a typical upward-downward trend in the face of increasing reaction severity. At 220 °C, 5-HMF occupies the highest fraction of the liquid phase with around 54.1 mg/g_{bio}, while at 250 °C it drops to 10.9 mg/g_{bio} probably due to its competing polymerization/polycondensation to form carbonaceous microspheres and rehydration reactions to carboxylic acids (Falco et al., 2011; Gong et al., 2022). Under the investigated conditions, the maximum conversion of biomass to 5-HMF is 5.4 wt%, which agrees with the literature (Becker et al., 2014). Furfural is almost

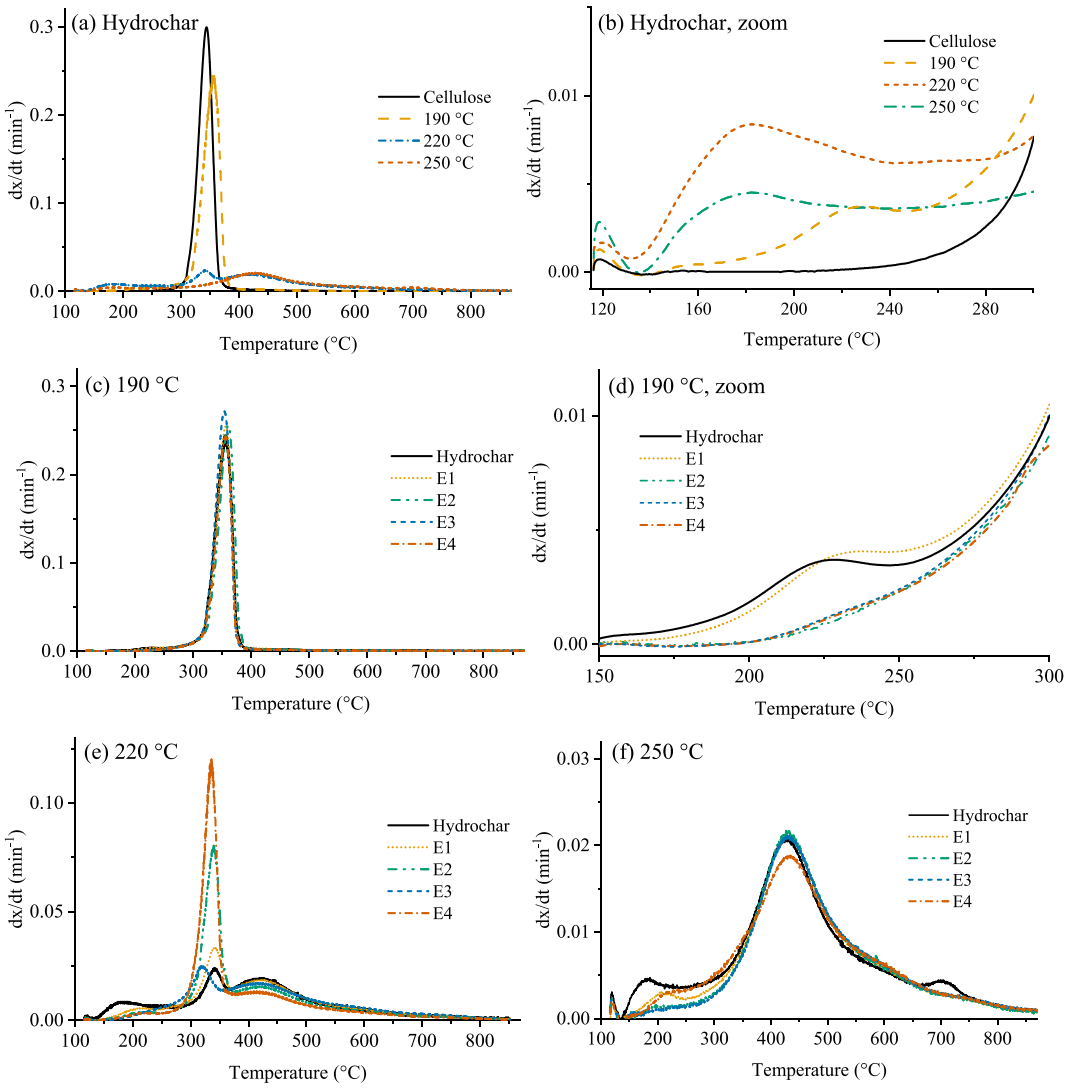

Fig. 1. DTG curves of: (a-b) hydrochars from cellulose at different HTC temperatures; (c-f) non-extractable hydrochars from cellulose resulting from the different extractions.

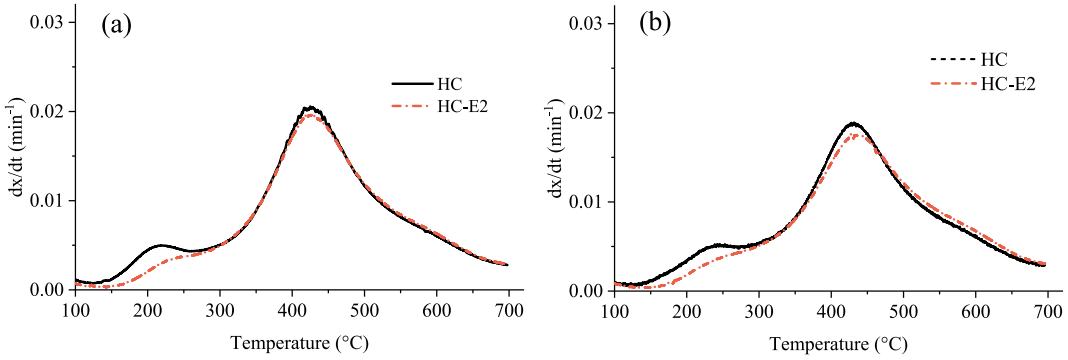

Fig. 2. DTG curves of hydrochars (HC) from glucose and their fractions remained after extraction E2 (HC-E2). For details on HC from glucose refer to Ischia et al. (2022).

absent in the HTC liquor produced at 190 °C and achieves a yield of 3.3 mg/g_{bio} at 220 and 250 °C as a result of the reverse aldol condensation of fructose.

Small amounts of ketones form at 220 and 250 °C from the cyclization of fragments released by hydrolysis, while phenols derive from the degradation of furfurals and aldehydes/unsaturated intermediates (González Martínez et al., 2018; Toor et al., 2011).

The measured TOC of the HTC liquor (Table 2) varies from 4.3 to 35.2 to 20.7 g/L at HTC temperatures of 190, 220 and 250 °C, respectively. The lowest value of TOC at 190 °C is due to the aforementioned low solubility of cellulose and minimal hydrolysis at this condition. The decrease in TOC from 220 to 250 °C is likely due to compounds dissolved

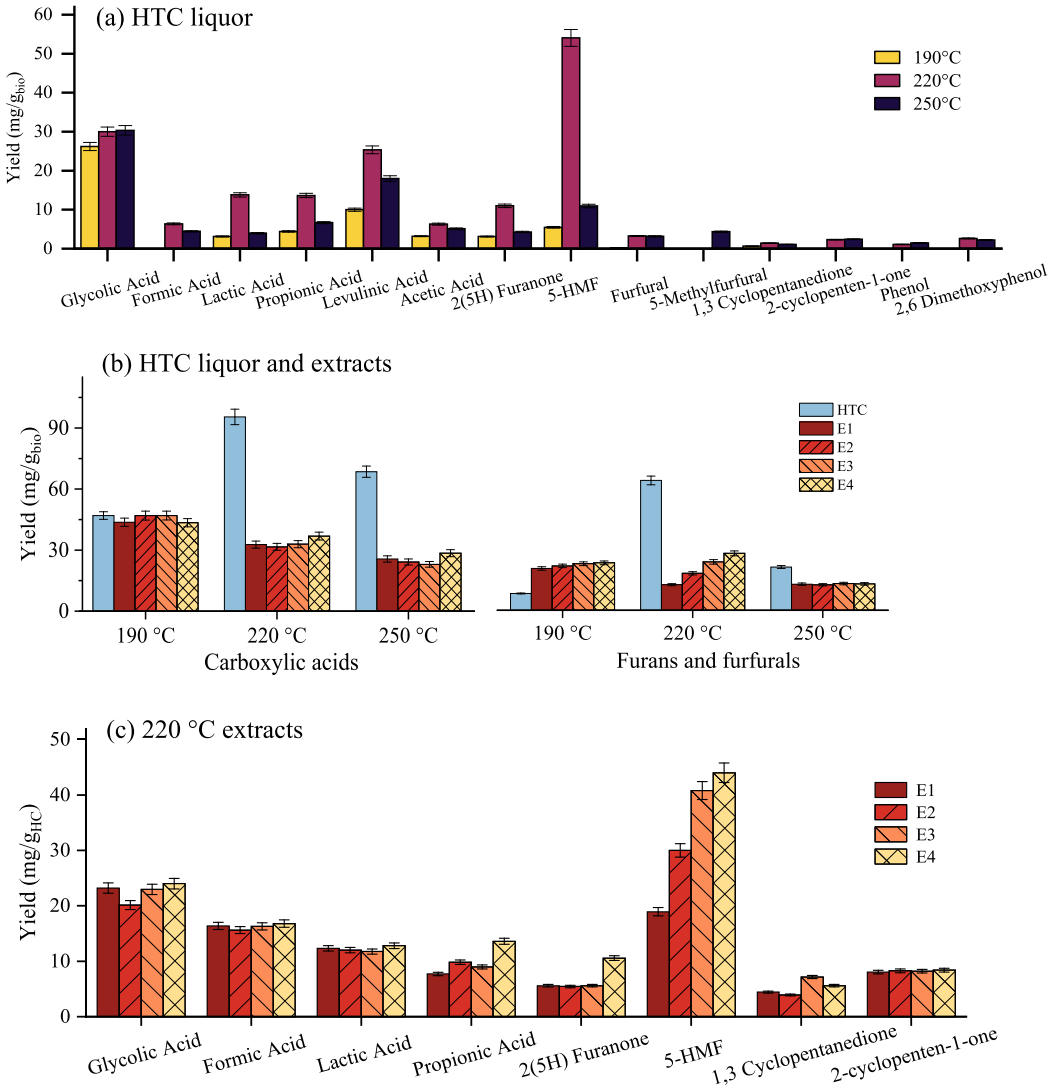

Fig. 3. HPLC liquid phase composition of: (a) HTC liquor at different temperatures (in mg/g_{bio}); (b) comparison between carboxylic acids and furans and furfurals in the HTC liquor and extracts (in mg/g_{bio}); (c) extracts from 220 °C hydrochar (in mg/g_{HC}) (in Supplementary Information the 190 and 250 °C cases).

Table 2
TOC of the HTC liquor (measured and computed from HPLC detected compounds) and liquid yields computed by weight difference (100-solid yield-gas yield) and HPLC data.

	HTC		
	190 °C	220 °C	250 °C
TOC (g/L)	4.3 ± 0.3	35.2 ± 1.5	20.7 ± 1.1
TOC_{HPLC} (g/L)	4.8 ± 0.2	16.7 ± 0.6	9.2 ± 0.4
Liquid yield (wt %)	7.4 ± 0.9	39.4 ± 0.9	43.2 ± 1.9
Liquid yield HPLC (wt %)	5.6 ± 0.2	17.1 ± 0.7	9.9 ± 0.4

into the liquid phase forming secondary char and the higher gas production. We note that there is no statistically significant difference between the elemental carbon content of the HCs produced at 220 and 250 °C ($p > 0.3$), but the increase in gas yield between these two data points is highly statistically significant ($p < 0.01$), such that the conversion of hydrolyzed compounds to CO_2 at higher HTC temperatures is likely the driving force behind the lower TOC at 250 °C.

The TOC computed from HPLC data (given by the sum of the carbon of all the detected compounds) agrees with the upward-downward trend of the measured TOC, but they differ substantially at the two highest temperatures (e.g., 20.7 vs 9.2 g/L at 250 °C, Table 2). A similar discrepancy is observed in the liquid mass yields computed from the mass balance and those estimated from HPLC data (Table 2). Therefore, HPLC data does not measure the entire liquid composition. Given the complexity of the HTC liquor, this discrepancy is likely related to a large number of dissolved compounds that are not detected via HPLC. This includes (1) compounds in non-identified peaks, (2) HTC-produced water not measurable by HPLC, and (3) the presence of carbonaceous micro/nanoparticles with diameters lower than 2.5 μm, comprising the colloidal fraction, that are not measurable via HPLC.

3.3. *Effect of solvent extraction on the hydrochars*

Cellulose's highly polymerized structure consisting of inter- and intramolecular hydrogen bonds infers stability and insolubility in all investigated solvents (Klemm et al., 2005), which in turn ensures the isolation of compounds formed during HTC. In addition, for all hydrochars, no mass loss is measured after extraction with *n*-hexane, indicating that the extractable phase is devoid of (detectable) non-polar compounds. The absence of non-polar compounds is likely due to the polar nature of cellulose, rich in oxygenated functionalities that tend to form polar compounds, as well as the mild temperature and heating

rates of HTC, not favoring the bio-oil production. The *n*-hexane extraction indicates the absence of a hydrophobic layer adsorbed on the hydrochar surface consisting of non-polar compounds, which was previously observed in the literature (Fan et al., 2022). The presence of such a non-polar layer depends on the feedstock. For example, a high-lipid feedstock forms fatty acid that adsorb on the hydrochar surface, whereas the cellulose used here is unable to form such compounds (Fan et al., 2022; Ischia et al., 2021; Wüst et al., 2020).

Extraction results vary with solvent and hydrochar. As mentioned in Section 3.1, microspheres forming secondary char are qualitatively unaffected by the extraction (Supplementary Information) and hydrochars from glucose present also stage I that is partially removed through the extraction (Fig. 2).

Extractions mildly affect the 190 °C hydrochar, whose extraction solid yields are 93.0–95.5 wt% (Table 1). The composition (Table 1) and thermal profiles of the non-extractable hydrochars (Fig. 1c-d) vary only slightly from the original hydrochar. Extraction with ethyl acetate alone does not alter the hydrochar DTG curves, suggesting the predominance of polar compounds adsorbed on the hydrochar surface (as ethyl acetate is the least polar solvent of those investigated). Stage I of the DTG curves is reduced after E2, E3, and E4, indicating the effectiveness of these extractions in removing more volatile, thermally unstable (and likely reactive) species.

The 220 °C hydrochar is significantly affected by all extractions, with solid yields of 72.0–92.0 wt% (Table 1). Among the extractions, E1 leads to the lowest extraction yield (8.0 wt%). E2 yields 15.0 wt% of extracted material, while using the three solvents combined or in sequential order (E3 and E4) extracts 26.0–28.0 wt% (difference between E3 and E4 not statistically significant). E3 and E4 result in 31.5–38.2 % of the C contained into the solid phase removed to the solvent phase (Table 1: CL values). The high mass loss seen with E3 and E4 of the 220 °C hydrochar compared to both E1 and E2 and the other hydrochars accords with the wider variety of mobile compounds present in the liquid phase (which are then adsorbed onto the hydrochar surface) at 220 °C. The 220 °C HTC liquor shows the highest amount of dissolved carbon (Table 2), suggesting a greater amount of potentially adsorbable compounds on the hydrochar. While not all of the dissolved compounds are identified through HPLC, the HPLC spectra of the liquor and the E3 and E4 extracts present the same undefined peaks (at retention times greater than 6 min, Supplementary Information), indicating that some undefined compounds of the HTC liquor undergo adsorption but can be extracted only through E3 and E4. Since non-polar compounds are absent (as shown by *n*-hexane extractions), these undefined compounds should be polar and/or slightly polar. Being that 220 °C is an intermediate condition at which unreacted cellulose, reacted cellulose, and secondary char coexist, it seems reasonable that the undefined dissolved fraction would contain intermediates deriving from the partial dissolution/hydrolysis of cellulose and compounds derived from the dissolution of partially formed nano/microparticles. Prior research demonstrates that increasingly harsh HTC of cellulose enhances the acidic and oxygenated surface functional groups (Saha et al., 2019). These surface functionalities, deriving from the unreacted cellulose and surface oxidization of the biomass, may serve as adsorption sites for the polar/slightly polar dissolved compounds.

The 250 °C hydrochars give up less extractable matter to all solvents than their lower-temperature counterparts, with extraction solid yields of 90.0–91.5 wt%. HPLC quantifies almost all the amount of extractable material, as shown by the slight discrepancy between extraction yields computed by weight measures and, for comparison, by the sum of HPLC-detected compounds (Supplementary Information). The overall lower extraction yields compared to the 220 °C hydrochar is attributed to a two-part mechanism. First, the higher conversion of cellulose to more cyclic/aromatic components with fewer cellulose intermediaries means that there are fewer readily adsorbable compounds dissolved in the liquid phase (they form into the liquid but do not undergo adsorption). Second, as HTC temperature increases, the hydrochar sees a decrease in its oxygenated surface character, making it less able to adsorb polar compounds (Saha et al., 2019).

Overall, the relative composition of the washed hydrochars slightly varies from the starting hydrochars (Table 1). Consistently with the extraction yields, the C trends slightly vary for the 190 and 250 °C cases – with around 93.6–97.0 % and 87.6–91.9 % of the C inside the hydrochar remaining into the solid phase (Table 1: CL values). However, for the 190 and 250 °C cases, none of the CL values are statistically significantly dependent on the extraction solvent/method used. The high dissolution effect of E3 and E4 on the 220 °C hydrochar results in a CL of 31.5–38.2 % (very statistically significantly different than E1 and E2; $p < 0.05$); the washed hydrochars are not statistically significantly different than the hydrochar in terms of their O/C and H/C ratios ($p > 0.05$). This suggests that while E3 and E4 are more efficient at extracting carbonaceous components, they do not selectively remove compounds based on functional groups. This further indicates that the adsorption of the compounds to the hydrochar is physical in nature given this desorption.

Solvent extraction shifts the thermal profile of the hydrochars by removing the thermally unstable species on their surface, aligning the thermal profiles of the extracted hydrochars with those of low-rank coals. This could be advantageous for co-combustion applications (Nguyen et al., 2022). However, enthusiasm for this solution must be tempered, as although the thermal stability of hydrochar increases, solvent extractions result in slight variation in elemental composition and therefore energy content as shown by the HHVs (maximum at 250 °C with 24.3–25.5 MJ/kg). A low ash content is crucial for maintaining a high energy content since it avoids the concentration of inert material in the hydrochars (and, therefore, the relative reduction of organic combustible material). Further research is undoubtedly needed to probe the combustion behavior (Nguyen et al., 2022). Practically, the costs and availability of the solvents should be considered to move forward with industrial-scale applications. Recirculating solvents back until saturation could reduce the consumption of raw materials and optimize costs. Organics dissolved in the solvents could be recovered as by-products and the solvent then recycled in the process. Future work could include a life cycle-technoeconomic analysis to evaluate this biorefinery's scalability and to guide decision making on a cost-benefit basis of other green solvents.

3.4. Composition of the extracts

The extracts' composition resembles that of the HTC liquor, with the number of compounds increasing with the HTC temperature (Fig. 3c and Supplementary Information). Extracts mainly contain carboxylic acids (formic, glycolic, and propionic acids) and furans (5H-furanone and 5-HMF), with smaller traces of ketones and phenols derivatives only in the 220 and 250 °C samples. All the identified compounds are rich in hydroxyl and carboxylic groups and have partition coefficients (logP) lower than two ("PubChem," n.d.), indicating a low level of hydrophobicity and high solubility in polar solvents.

The similarity between the extract and the liquor composition suggests that extracted organics derive from the liquor itself and are adsorbed on the hydrochar surface during HTC and/or the filtration downstream HTC. Fig. 3b shows that the amounts of extracted compounds (divided by family and referred to as per g of cellulose) are comparable to those in the HTC liquor. Their distribution as adsorbed/dissolved fractions depends on the HTC temperature. Therefore, the solid phase has a notable "sink" capacity for dissolved compounds and could be used to maximize the recovery of platform chemicals. At 190 °C, carboxylic acids are equally distributed among the solid and liquid phases, while furans and furfurals are mostly adsorbed on the hydrochar. This could be due to the higher affinity of the 190 °C hydrochar, rich in polar functionalities deriving from the cellulose itself, with the high polarity of these compounds, which are easily adsorbed. At 220 °C, polar compounds are found mostly in the liquor phase, probably

due to the lower adsorption capacity of the solid phase.

The amount of each extracted compound (in mg/g_{HC}) slightly varies with the extraction type and operating condition (Fig. 3c and Supplementary Information). Carboxylic acids occupy the main fraction of the extracts (>50 wt%) and their amount slightly changes with the extraction type, with values of 47.3–67.2 mg/g_{HC} (i.e., they compose 4.7–6.7 % of the hydrochars). Since carboxylic acids are highly soluble in polar solvents, it seems plausible that extractions are capable of entirely removing them. Resembling the HTC liquor trend, 220 °C exhibits the maximum yield of 5-HMF. In this case, the type of extraction affects the removal yield, with E3 and E4 extracting up to 40.8 and 44.0 mg/g_{HC} of HMF, respectively. 5-HMF is a less polar chemical (also soluble in some non-polar compounds, like chloroform), and therefore the wider solvent properties (like polarity, hydrogen bonding, and molecular size) covered by E3 and E4 with respect to E1 and E2 is conducive to 5-HMF extraction. The 190 and 250 °C cases do not show this dependence (Supplementary Information), with extracts having a constant concentration, likely due to the generally lower amount of 5-HMF itself. Two key takeaways emerge here: first, that extraction type only slightly influences the extracts' composition. Second, the similarity between extraction yields as computed by mass balance and HPLC for the 190 and 250 °C hydrochars (Supplementary Information) highlights the interchangeable nature of the solvents in terms of overall and specific compounds recovery. The similarity is not observed for the 220 °C, where HPLC does not allow for closure of the balance (Supplementary Information) for E3 and E4, opening the doors to further investigations on the non-detected adsorbable compounds.

3.5. Effect of solvents on solubility and hydrochars

The effect of solvents can be broken into two categories: effects on component solubility and on extraction process. The extraction effectiveness depends on the solubility of components embedded with the hydrochar matrix and the solvent used. Polar or slightly polar solvents interact favorably with =O, –OH and –COOH groups of adsorbed compounds, easily extracting carboxylic acids, furans, phenols, and ketones. Polarity appears to be the main driver for the dissolution, especially for the 190 and 250 °C chars (where differences among the extraction media are almost negligible).

Other properties like hydrogen bonding and molecular size can participate directly or indirectly in the dissolution. For example, carboxylic acids are soluble due to their polarity and hydrogen bonding tendency conferred by their carboxylic groups, while carbonyl groups in detected ketones contribute polarity aiding their dissolution. In the 220 °C case, the significantly higher efficacy of E3/E4 than E1/E2 likely stems from the broader range of solvent properties. E3 benefits from the initial use of ethyl acetate, which extracts moderately polar and larger components owing to its larger molecular size, while the subsequent acetone/methanol mixture potentially generates hydrogen bonding sites due to the carbonyl and hydroxyl groups and promotes the solubility of smaller molecules due to their smaller size. E4, in contrast, offers efficient solubilization by simultaneously differentiating solvent properties and providing access to all three solvents, maximizing hydrogen bonding potential. For instance, the higher solubility of both 5-HMF and 2(5H)-furanone is likely due to the simultaneous presence of bond donors and acceptors in the ternary mixture. Future studies might involve alternative solvents to discern the effects of polarity on adsorbed species and gain further mechanistic insights.

The extraction process is driven by the interaction between solvents and hydrochar, where solvent molecules penetrate the hydrochar matrix and dissolve the adsorbed compounds from the surface to the solvent, altering the hydrochar's composition and properties. As adsorbed compounds are removed, hydrochar's properties are redistributed, with hydrochar's elemental ratios and thermal stability modulated by the solvents. All the investigated extractions positively affect the hydrochar's thermal profiles. Resembling the solubility behavior observations, only the 220 °C composition is affected by the solvent type, with E3/E4 resulting in the highest carbon mass losses (up to 38.2 %). Future work may expand upon the present findings concerning how manipulating the polarity of solvent mixtures may maximize hydrochar extraction. At the same time, analyses of the surface chemistry of the hydrochars could provide insight into the mechanisms behind the adsorption and the effects of extraction. In addition, because carboxylic acids and furans present in hydrochar may be phytotoxic or leach into groundwater (Karatas et al., 2022), their removal is particularly relevant for environmental applications. Future work could investigate how solvent extraction mitigates plant, animal, and human health risks when using these materials as soil amendments, carbon sequestration materials, and environmental adsorbents.

Finally, it is worth noting that the scope of this work was limited to cellulose as a representative carbohydrate compound. Since the impact of extraction and the variety of extracted compounds highly depends on the feedstock, future research could focus on other crucial biomass components characterized by different chemistries. Indeed, lignin-based feedstocks lead to a high amount of phenol derivatives (Lin et al., 2022; Toor et al., 2011), while lipid-rich substrates (like organic wastes or algae) to fatty acids (Benavente et al., 2022; Ischia et al., 2021; Wu et al., 2020).

4. Conclusion

Green polar solvents can effectively remove surface-adsorbed organics from cellulosic hydrochars. The extract composition resembles the HTC liquor and consists of carboxylic acids, furans, phenols, and ketones, supporting the hypothesis that adsorbed compounds on the hydrochar are responsible for hydrochar's poor thermal stability. The washed hydrochars do not contain these compounds and are likely more usable in combustion or environmental applications, while extracted compounds could be recovered as fuel precursors. Stable secondary char consisting of carbonaceous microspheres remains unaffected by the extraction with polar solvents.

CRediT authorship contribution statement

Giulia Ischia: Conceptualization, Data curation, Formal analysis, Investigation, Methodology, Visualization, Writing – original draft. **Jillian L. Goldfarb:** Conceptualization, Project administration, Resources, Writing – review & editing. **Antonio Miotello:** Resources, Supervision, Writing – review & editing. **Luca Fiori:** Conceptualization, Project administration, Resources, Supervision, Writing – review & editing.

Declaration of Competing Interest

The authors declare the following financial interests/personal relationships which may be considered as potential competing interests: Giulia Ischia reports financial support was provided by The US-Italy Fulbright Commission. Jillian L. Goldfarb reports financial support was provided by USDA National Institute of Food and Agriculture. Jillian L. Goldfarb reports financial support was provided by U.S. National Science Foundation. Jillian L. Goldfarb reports a relationship with Bioresource Technology that includes: board membership.

Data availability

Data will be made available on request.

Acknowledgments

Giulia Ischia was financially supported by the U.S.-Italy Fulbright Commission. We thank the financial support provided by the ERICSOL project of the University of Trento. This work was partially supported by a Hatch Grant under accession number 1021398 from the USDA

National Institute of Food and Agriculture, U.S., and by the U.S. National Science Foundation under grant CBET-2031710. The authors thank N. Bazzanella (University of Trento) for assistance with SEM image acquisition, C. Gavazza and Prof. L. Fambri (University of Trento) for assistance with the thermogravimetric analyses on hydrochars from glucose, and H. Sudibyo and J.W. Tester (Cornell University) for assistance with the ultimate analysis.

Appendix A. Supplementary data

Supplementary data (includes expanded yield data, HPLC analysis, and SEM images) to this article can be found online at https://doi.org/10.1016/j.biortech.2023.129724.

References

Arauzo, P.J., Lucian, M., Du, L., Olszewski, M.P., Fiori, L., Kruse, A., 2020a. Improving the recovery of phenolic compounds from spent coffee grounds by using hydrothermal delignification coupled with ultrasound assisted extraction. Biomass Bioenergy 139, 105616. https://doi.org/10.1016/j.biombioe.2020.105616.

Arauzo, P.J., Olszewski, M.P., Wang, X., Pfersich, J., Sebastian, V., Manyà, J., Hedin, N., Kruse, A., 2020b. Assessment of the effects of process water recirculation on the surface chemistry and morphology of hydrochar. Renew. Energy 155, 1173–1180. https://doi.org/10.1016/J.RENENE.2020.04.050.

Becker, R., Dorgerloh, U., Paulke, E., Mumme, J., Nehls, I., 2014. Hydrothermal carbonization of biomass: Major organic components of the aqueous phase. Chem. Eng. Technol. 37, 511–518. https://doi.org/10.1002/ceat.201300401.

Benavente, V., Lage, S., Gentili, F.G., Jansson, S., 2022. Influence of lipid extraction and processing conditions on hydrothermal conversion of microalgae feedstocks – Effect on hydrochar composition, secondary char formation and phytotoxicity. Chem. Eng. J. 428, 129559 https://doi.org/10.1016/j.cej.2021.129559.

Byrne, F.P., Jin, S., Paggiola, G., Petchey, T.H.M., Clark, J.H., Farmer, T.J., Hunt, A.J., Robert McElroy, C., Sherwood, J., 2016. Tools and techniques for solvent selection: green solvent selection guides. Sustain. Chem. Process. 4, 1–24. https://doi.org/10.1186/s40508-016-0051-z.

Cao, Y., He, M., Dutta, S., Luo, G., Zhang, S., Tsang, D.C.W., 2021. Hydrothermal carbonization and liquefaction for sustainable production of hydrochar and aromatics. Renew. Sustain. Energy Rev. 152, 111722 https://doi.org/10.1016/j.rser.2021.111722.

Falco, C., Baccile, N., Titirici, M.M., 2011. Morphological and structural differences between glucose, cellulose and lignocellulosic biomass derived hydrothermal carbons. Green Chem. 13, 3273–3281. https://doi.org/10.1039/c1gc15742f.

Fan, J., Li, F., Fang, D., Chen, Q., Chen, Q., Wang, H., Pan, B., 2022. Effects of hydrophobic coating on properties of hydrochar produced at different temperatures: Specific surface area and oxygen-containing functional groups. Bioresour. Technol. 363, 127971 https://doi.org/10.1016/J.BIORTECH.2022.127971.

Gao, L., Volpe, M., Lucian, M., Fiori, L., Goldfarb, J.L., 2019. Does hydrothermal carbonization as a biomass pretreatment reduce fuel segregation of coal-biomass blends during oxidation? Energy Convers. Manag. 181, 93–104. https://doi.org/10.1016/j.enconman.2018.12.009.

Gong, Y., Xie, L., Chen, C., Liu, J., Antonietti, M., Wang, Y., 2022. Bottom-up hydrothermal carbonization for the precise engineering of carbon materials. Prog. Mater. Sci. 132, 101048 https://doi.org/10.1016/j.pmatsci.2022.101048.

González Martínez, M., Dupont, C., Thiéry, S., Meyer, X.M., Gourdon, C., 2018. Impact of biomass diversity on torrefaction: Study of solid conversion and volatile species formation through an innovative TGA-GC/MS apparatus. Biomass Bioenergy 119, 43–53. https://doi.org/10.1016/j.biombioe.2018.09.002.

He, M., Zhu, X., Dutta, S., Khanal, S.K., Lee, K.T., Masek, O., Tsang, D.C.W., 2022. Catalytic co-hydrothermal carbonization of food waste digestate and yard waste for energy application and nutrient recovery. Bioresour. Technol. 344, 126395 https://doi.org/10.1016/j.biortech.2021.126395.

Ischia, G., Fiori, L., Gao, L., Goldfarb, J.L., 2021. Valorizing municipal solid waste via integrating hydrothermal carbonization and downstream extraction for biofuel production. J. Clean. Prod. 289, 125781 https://doi.org/10.1016/j.jclepro.2021.125781.

Ischia, G., Cutillo, M., Guella, G., Bazzanella, N., Cazzanelli, M., Orlandi, M., Miotello, A., Fiori, L., 2022. Hydrothermal carbonization of glucose: Secondary char properties, reaction pathways, and kinetics. Chem. Eng. J. 449, 137827 https://doi.org/10.1016/j.cej.2022.137827.

Kang, S., Li, X., Fan, J., Chang, J., 2012. Characterization of hydrochars produced by hydrothermal carbonization of lignin, cellulose, d-xylose, and wood meal. Ind. Eng. Chem. Res. 51, 9023–9031. https://doi.org/10.1021/ie300565d.

Karatas, O., Khataee, A., Kalderis, D., 2022. Recent progress on the phytotoxic effects of hydrochars and toxicity reduction approaches. Chemosphere 298, 134357. https://doi.org/10.1016/j.chemosphere.2022.134357.

Klemm, D., Heublein, B., Fink, H.P., Bohn, A., 2005. Cellulose: Fascinating biopolymer and sustainable raw material. Angew. Chem., Int. Ed. 44, 3358–3393. https://doi.org/10.1002/anie.200460587.

Kruse, A., Zevaco, T.A., 2018. Properties of hydrochar as function of feedstock, reaction conditions and post-treatment. Energies 11, 1–12. https://doi.org/10.3390/en11030674.

Lin, H., Li, Q., Zhang, S., Zhang, L., Hu, G., Hu, X., 2022. Involvement of the organics in aqueous phase of bio-oil in hydrothermal carbonization of lignin. Bioresour. Technol. 351, 127055 https://doi.org/10.1016/J.BIORTECH.2022.127055.

Lucian, M., Volpe, M., Gao, L., Piro, G., Goldfarb, J.L., Fiori, L., 2018. Impact of hydrothermal carbonization conditions on the formation of hydrochars and secondary chars from the organic fraction of municipal solid waste. Fuel 233, 257–268. https://doi.org/10.1016/j.fuel.2018.06.060.

Modugno, P., Titirici, M.M., 2021. Influence of reaction conditions on hydrothermal carbonization of fructose. ChemSusChem 14 (23), 5271–5282. https://doi.org/10.1002/cssc.202101348.

Nguyen, D., Zhao, W., Mäkelä, M., Alwahabi, Z.T., Kwong, C.W., 2022. Effect of hydrothermal carbonisation temperature on the ignition properties of grape marc hydrochar fuels. Fuel 313, 122668. https://doi.org/10.1016/j.fuel.2021.122668.

Nicolae, S.A., Au, H., Modugno, P., Luo, H., Szego, A.E., Qiao, M., Li, L., Yin, W., Heeres, H.J., Berge, N., Titirici, M.M., 2020. Recent advances in hydrothermal carbonisation: From tailored carbon materials and biochemicals to applications and bioenergy. Green Chem. 22, 4747–4800. https://doi.org/10.1039/d0gc00998a.

Pecchi, M., Baratieri, M., Goldfarb, J.L., Maag, A.R., 2022. Effect of solvent and feedstock selection on primary and secondary chars produced via hydrothermal carbonization of food wastes. Bioresour. Technol. 348, 126799 https://doi.org/10.1016/j.biortech.2022.126799.

Poerschmann, J., Weiner, B., Koehler, R., Kopinke, F.D., 2017. Hydrothermal carbonization of glucose, fructose, and xylose - identification of organic products with medium molecular masses. ACS Sustain. Chem. Eng. 5, 6420–6428. https://doi.org/10.1021/acssuschemeng.7b00276.

PubChem, URL https://pubchem.ncbi.nlm.nih.gov/ (accessed 3.24.23).

Saha, N., Saba, A., Reza, M.T., 2019. Effect of hydrothermal carbonization temperature on pH, dissociation constants, and acidic functional groups on hydrochar from cellulose and wood. J. Anal. Appl. Pyrolysis 137, 138–145. https://doi.org/10.1016/j.jaap.2018.11.018.

Toor, S.S., Rosendahl, L., Rudolf, A., 2011. Hydrothermal liquefaction of biomass: A review of subcritical water technologies. Energy 36, 2328–2342. https://doi.org/10.1016/j.energy.2011.03.013.

Wu, K., Zhang, X., Yuan, Q., Liu, R., 2020. Investigation of physico-chemical properties of hydrochar and composition of bio-oil from the hydrothermal treatment of dairy manure: Effect of type and usage volume of extractant. Waste Manag. 116, 157–165. https://doi.org/10.1016/j.wasman.2020.08.004.

Wüst, D., Correa, C.R., Jung, D., Zimmermann, M., Kruse, A., Fiori, L., 2020. Understanding the influence of biomass particle size and reaction medium on the formation pathways of hydrochar. Biomass Convers. Biorefinery 10, 1357–1380. https://doi.org/10.1007/s13399-019-00488-0.

Yilmaz, E., Soylak, M., 2020. Type of green solvents used in separation and preconcentration methods. In: New Generation Green Solvents for Separation and Preconcentration of Organic and InOrganic Species. Elsevier, pp. 207–266.